

1-1-1998

Alpha Particle Fragments Produced From Multifragmentation of $^{16}\text{O}+^{16}\text{O}$

M.Y.H. FARAG

Follow this and additional works at: <https://journals.tubitak.gov.tr/physics>



Part of the [Physics Commons](#)

Recommended Citation

FARAG, M.Y.H. (1998) "Alpha Particle Fragments Produced From Multifragmentation of $^{16}\text{O}+^{16}\text{O}$," *Turkish Journal of Physics*: Vol. 22: No. 1, Article 4. Available at: <https://journals.tubitak.gov.tr/physics/vol22/iss1/4>

This Article is brought to you for free and open access by TÜBİTAK Academic Journals. It has been accepted for inclusion in Turkish Journal of Physics by an authorized editor of TÜBİTAK Academic Journals. For more information, please contact academic.publications@tubitak.gov.tr.

Alpha Particle Fragments Produced From Multifragmentation of $^{16}\text{O} + ^{16}\text{O}$

M.Y.H. FARAG

*Physics Department, Faculty of Science
Cairo-EGYPT*

Received 09.07.1996

Abstract

Angular distribution for alpha particles produced from multifragmentation of $^{16}\text{O} + ^{16}\text{O}$ reactions are calculated using the statistical scission model. The alpha particles are sequentially emitted from long lived states of primary fragments populated in these reactions. Eight alpha particles are produced in these reactions. The calculations are carried out for different energies and for different nuclear temperatures. The variances of this multifragmentation process have been numerically calculated. The obtained results are in good agreement with previous calculations.

1. Introduction

In nucleus-nucleus collisions at low energies ($E_{proj} \leq 10\text{MeV/nucleon}$), the dominant reaction mechanism shifts [1] from complete fusion to deep inelastic scattering as long as the projectile charge and size increase. The complete fusion cross sections for collision of heavy nuclei at low energies are expected [2] to be zero. While the collision of the light medium heavy ions with heavy nuclei is a transition from complete fusion to incomplete fusion to spallation like or multifragmentation reaction mechanisms as the projectile energy increases from 10 to 100 MeV/nucleon. At low energies the strong Coulomb repulsion prevents [1] the deeper penetrations of target and projectile nuclei that lead to fusion like events. However, the complete fusion between heavy ions is considered as a complete (fusion between heavy ions is considered as a complete) amalgamation of all the nucleons of the target and projectile into a composite system formed [3] inside the fission barrier. This process in case of systems leading to nonfissioning nuclei is identified either by direct observation of the residue of the fused system after thermal evaporation of particles or by observation of the characteristic gamma rays from the final steps of the decay process. These observations may be good signatures [3] for complete fusion except

at higher beam velocities where the emission of fast particles from the interacting ions prior to fusion may not be excluded experimentally. Fission like products with symmetric masses may be obtained from reactions with typical characteristics of a direct process, without proceeding through a step of complete fusion. The angular distributions of fragments from the fission decay of compound nuclei formed by complete fusion reactions with heavy ion projectiles are consistent with those expected on the basis of the saddle point model of fission. This model is based on the assumption that the distribution is unchanged during the descent from the saddle to the scission point. The saddle point model introduces a good account of the angular distributions which well justified this assumption [3], even in the case of high temperatures and angular momenta. According to the transition state theory, the saddle point in the potential energy surface for nuclear shape degrees of freedom represents a distinct point in the fission trajectory where the direction of the fission axis with respect to the nuclear spin was determined. The fissioning nucleus at relatively low excitation energies attains a thermal equilibrium at this stationary point, populating statistically transition states whose structure is well determined by the values of the collective shape and spin parameters at the saddle point. This shows that the statistical transition model provides a good representation of the experimental angular distributions of fragments from low energy fission of nuclei with finite barriers and well defined transition state configurations. It is also assumed that the spin projection on the nuclear symmetry axis remains [4] unchanged during any subsequent descent from the saddle to scission points.

However, the various directions of the fission axis of the axially symmetric nucleus in the statistical transition model are assumed to be populated according to the density of the intrinsic transition states. These directions depend on the moments of inertia of the collective rotations about its principle axes and the nuclear temperature. The moments of inertia are related [5] to the spin dependent saddle point shapes predicted by the rotating liquid drop model which are axially symmetric for lighter systems and are triaxial for heavy nuclei. The transition state theory is inapplicable for nuclear spins which are excess of the rotating liquid drop model limit of stability, where an equilibrium point in the potential energy no longer exists. It is also may be inapplicable for cases [6] when the nuclear temperature exceeds magnitudes which are equivalent to the height of the fission barrier. The fission fragment angular distributions for reactions between heavy systems with smaller negligible fission barriers, are calculated [4] with statistical scission model [7]. This model is also realistic when the angular momentum and excitation energy are large. In the scission point model, the distribution of the spin projection is readjusted [3] adiabatically during the descent from saddle to scission such that the fission anisotropy reflects a statistical distribution of the spin projectile values at the scission point. The prediction of the scission point model is introduced [8] as that the distribution of the final spin projection values is estimated from the distribution of the channel spin. Thus the scission point configuration is assumed [8] to be consistent with the observed total kinetic energies in fission. However, the channel spin distribution is estimated on the basis of the fragment moments of inertia perpendicular to the symmetry axis.

In the present work, we study the $^{16}\text{O} + ^{16}\text{O}$ reactions at different energies in a multifragmentation process, leading to emission of rigid alpha particles. The outgoing particles in this reaction are eight alpha particles. The fission fragment angular distributions are developed using the statistical scission model. Theoretical expressions are introduced for the cross sections of the fission fragments. Numerical calculations are carried out for the cross sections and variances of the multifragmentation process.

The multifragmentation formalism of statistical scission model is introduced in section 2. The calculations and results are given in section 3. While the discussion and conclusions are presented in section 4.

2. Formalism

The angular dependence of fission decays in general may be expressed in terms of projection k of the total spin vector I on the center axis of the separated fission fragments which is normally denoted by the fission axis. When target and projectile spins are zero and the projection of the spin I on to the beam axis is zero throughout the fission process, $M = 0$, then the angular distribution of the fragments may be expressed [4] as

$$W(E, \theta) \propto \sum_{I,m} (2I+1) T_I \frac{\Gamma_f(E, I, m)}{\Gamma_f(E, I)} (I+1/2) |D_{0,m}^I(\theta)|^2, \quad (1)$$

where T_I are the transmission coefficients in the entrance channel for orbital angular momentum I . $D_{0,m}^I(\theta)$ are the normalized rigid rotor function. Also, we notice that

$$\Gamma_f(E, I) = \sum_m \Gamma_f(E, I, m), \quad (2)$$

where $\Gamma_f(E, I, m)$ is the relative fission decay width, which results as the product of the inverse cross section and density of the final states by using the reciprocity theorem. Therefore, we have

$$\Gamma_f(E, I, m) \propto \sum_{\ell, S} (2\ell+1) \exp\left[\frac{-E_R(\ell)}{T}\right] |\langle S m \ell O | I m \rangle|^2 \rho(E, S, m), \quad (3)$$

where $E_R(\ell)$ is the orbital rotational energy for angular momentum ℓ , μ is the reduced mass of fission channel and R_C is the distance between the centers of fission fragments at scission configuration. The energy is given by the equation

$$E_R(\ell) = \ell^2 \hbar^2 / 2\mu R_C^2. \quad (4)$$

The channel spin \vec{S} is the vector sum of the two fission fragment spins, so that $\vec{S} = \vec{i}_1 + \vec{i}_2$. The orbital angular momentum ℓ in the exit channel is perpendicular to the axis of the fission. The total energy E available at the scission configuration for $\ell = 0$ is then expressed as

$$E = E_{c.m.} + Q_{FF} - E_K - E_D - E_{PS}. \quad (5)$$

The different quantities given in equation (5) are $E_{c.m.}$ as the center of mass energy, Q_{FF} as the Q value for fission reaction, E_K as the total kinetic energy of the fission fragments for $\ell = 0$, E_D as the deformation energy of fission fragments and E_{PS} as the energy associated with precession particle emission. The total excitation energy of the two fragments including their thermal and intrinsic rotational energies is given by

$$E^* = E - E_R(\ell). \quad (6)$$

We should notice that the product $\rho(E, S, m) \exp[-E_R(\ell)/T]$ in equation (3) represents the intrinsic level density of the two fission fragments in a constant temperature level density formalism. One can, hence, identify the exponential factor in this product with the transmission coefficient $T_\ell \propto \exp[-E_R(\ell)/T]$ of the ℓ th partial wave in the exit channel. However, the spin dependent part, $\rho(S, m)$, of the state density $\rho(E, S, m)$ is given by

$$\rho(S, m) \propto (2S + 1) \exp[-(S + 1/2)^2/2(2\sigma^2)]. \quad (7)$$

The fission probability for a state in the composite nucleus with excitation energy E and spin I with projection m in the direction $\vec{n}(m = \vec{n} \cdot \vec{I})$ is given by the ratio of $\Gamma_f(E, I, m)/\Gamma(E, I)$, where $\Gamma(E, I)$ is the total decay width of the state with excitation energy E and spin I . This ratio can be rewritten as

$$\frac{\Gamma_f(E, I, m)}{\Gamma(E, I)} = \frac{\Gamma_f(E, I, m)}{\Gamma_f(E, I)} \frac{\Gamma_f(E, I)}{\Gamma(E, I)}. \quad (8)$$

The first part of the ratio on the right hand side of equation (8) $\Gamma_f(E, I, m)/\Gamma_f(E, I)$ appeared in equation (1), while the second part of the ratio $\Gamma_f(E, I)/\Gamma(E, I)$ takes the value of unity for values of I in the range $I_{\min} < I \leq I_{\max}$, and it takes the value of zero otherwise. Inserting the channel spin state density $\rho(S, m)$ given by equation (7) into equation (3) to perform the sums over orbital angular momentum ℓ and channel spin S , then we get for the spin dependent fission width ratio at a fixed excitation energy E the expression

$$\frac{\Gamma_f(E, I)}{\Gamma_f(I)} = \frac{\exp[-m^2/2S_0^2]}{\sum_{m'} \exp[-(m')^2/2S_0^2]}. \quad (9)$$

Then, by substituting equation (9) into equation (1), we get for a fixed excitation energy E , the following expression:

$$W(\theta) \propto \sum_{I_{\min}}^{I_{\max}} (2I + 1) T_\ell \frac{\sum_{m=-I}^I (I + 1/2) |D_{O,m}^I(\theta)|^2 e^{-m^2/2S_0^2}}{\sum_{m=-I}^I \exp(-m^2/2S_0^2)}. \quad (10)$$

The variance S_0^2 for spherical fission fragments is given by either of the following expressions

$$S_0^2 = \begin{cases} 2\sigma^2 \{ [2\sigma^2 + (\mu R_C^2 T/\hbar^2)] / (\mu R_C^2 T/\hbar^2) \} \\ (2I_0 T/\hbar^2) [(2I_0 + \mu R_C^2) / \mu R_C^2], \end{cases} \quad (11)$$

where

$$\sigma^2 = I_0 T / \hbar^2 = \frac{2}{5} M R^2 T / \hbar^2, \quad (12)$$

and I_0 is the moment of inertia; while M and R are the mass and radius of one of the symmetric fission fragments, respectively. T is the nuclear temperature. The value of R_C is given as $R_C = 1.438 Z_1 Z_2 / E_K$. Also, the temperature at scission is calculated from a relation [3] so that it has the expression

$$T_{scis} = \left[\frac{E_{c.m.} + Q_{FF} - E_K - E_D - E_{rot}}{A/8.5} \right]^{1/2}. \quad (13)$$

In equation (13), E_{rot} is the rotational energy of the scission configuration, A is the nuclear number, E_D is the energy bound in fragment deformation and E_K is the Viola estimate [9] of the total kinetic energy which is identified with the Coulomb repulsion energy at scission. The sum of the Coulomb and deformation energies is the energy stored in the potential energy at the instant of scission.

3. Calculations and Results

The statistical scission model is applied in the present work to nuclear fission. The angular distributions of fragments from oxygen induced fission are calculated. $^{16}O + ^{16}O$ reactions are considered. The products fission fragment particles are eight alpha particles. The more general formula for angular distributions which has been used [10] and found to work well for many cases of fission is that given by the expression of equation (10). The term $(2I + 1)T_\ell$ stands for the cross section of the formation of a specific compound nucleus with spin I . For formed compound nuclei with spin projection $m = 0$ along the beam direction, we can write that $\ell = I$, so that the transmission coefficients are written as T_ℓ instead of T_I . The factor $(I + 1/2)|D_{O,m}^I(\theta)|^2$ is the properly normalized angular distribution function for state of spin I and projection along the direction of emission m to decay into an angle θ to the beam direction. This function is given by an expression [11] as

$$(I + 1/2)^2 |D_{O,m}^I(\theta)|^2 \simeq \frac{1}{\pi} \frac{I + 1/2}{[(I + 1/2)^2 \sin^2 \theta - m^2]^{1/2}}. \quad (14)$$

The values of the variance S_0^2 are estimated [8] in the statistical scission model by $S_0^2 = \sigma_1^2 + \sigma_2^2$ for two fission fragments. The spin cutoff factors σ_i^2 are associated with the level densities of the two fission fragments. For the present work where there are more than two fission fragments, the variance S_0^2 is considered to be given by $S_0^2 = \Sigma \sigma_i^2$, where i is extended to all fission fragments. Therefore, we have

$$S_0^2 = 8\sigma^2. \quad (15)$$

The spin cutoff factor σ^2 is given by

$$\sigma^2 = \frac{2}{5} M R^2 T / \hbar^2. \quad (16)$$

In equation (16), M and R are the mass and the radius of the alpha particles while T is the nuclear temperature, which is related to the excitation energies E_i^* of the fragments by [11] $T \approx \frac{8}{A}[(E_{c.m.} + Q - E_K)]^{1/2}$ and is given [12] by the formula

$$T = \left[\frac{8}{A}(E_{c.m.} + Q - E_K) \right]^{1/2}. \quad (17)$$

In equation (17), A , $E_{c.m.}$, Q and E_K are the compound nucleus mass number, the center of mass bombarding energy, the Q value for the reaction channel leading to equal fission fragments and the average summed kinetic energies of the fragments, respectively. In the present work, the reaction is $^{16}\text{O} + ^{16}\text{O}$ leading to eight alpha particles. The Q value of this reaction is $Q = 28.871\text{MeV}$. The average summed kinetic energies E_K of the fragments is taken [9] systematically as the formula given by

$$E_K = \frac{0.107Z^2}{A^{1/3}} + 22 \text{ MeV}, \quad (18)$$

where A and Z are the mass and charge numbers of the compound nucleus, which are 32 and 16, respectively in the present work. Therefore, the calculated value of E_K is $E_K = 30.628\text{MeV}$. Then, the nuclear temperature T for different values of the bombarding energies can be given by using the above results, as given in Table 1, as calculated by using equation (17).

Table 1. Calculated angular distributions and variances

E_{lab} (MeV)	$E_{c.m.}$ (MeV)	T (MeV)	$W(\theta)/W(90)$					S_0^2 ($10^2\hbar^2$)
			$\theta = 10$	$\theta = 30$	$\theta = 50$	$\theta = 70$	$\theta = 90$	
70	35	2.883	6.751	2.166	1.441	1.088	1	3.340
80	40	3.092	6.707	2.170	1.445	1.090	1	3.582
90	45	3.288	6.665	2.173	1.449	1.091	1	3.810
100	50	3.473	6.625	2.177	1.453	1.093	1	4.024
110	55	3.648	6.586	2.179	1.456	1.094	1	4.227
120	60	3.816	6.549	2.182	1.459	1.096	1	4.421
130	65	3.976	6.514	2.184	1.462	1.097	1	4.607
140	70	4.130	6.480	2.186	1.465	1.098	1	4.785
150	75	4.279	6.447	2.188	1.468	1.099	1	4.958
160	80	4.423	6.415	2.189	1.471	1.101	1	5.125

The angular distribution $W(\theta)$ are calculated for various center of mass angles θ and various nuclear temperature T with values from $T = 1\text{MeV}$ to $T = 9\text{MeV}$. The results of these calculations are shown in Figure 1 for the transmission coefficient $T_\ell = 0.2$ and in Figure 2 for $T_\ell = 1.0$. The transmission coefficients that corresponding to the

FARAG

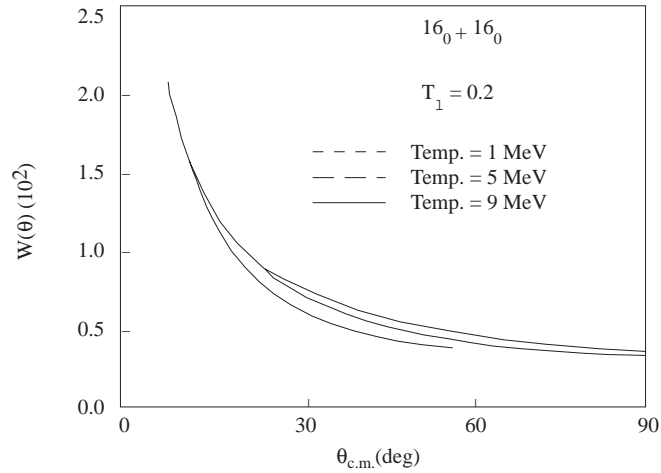


Figure 1. Angular distributions of alpha fragments from the $16_0 + 16_0$ reaction for various values of the nuclear temperature.

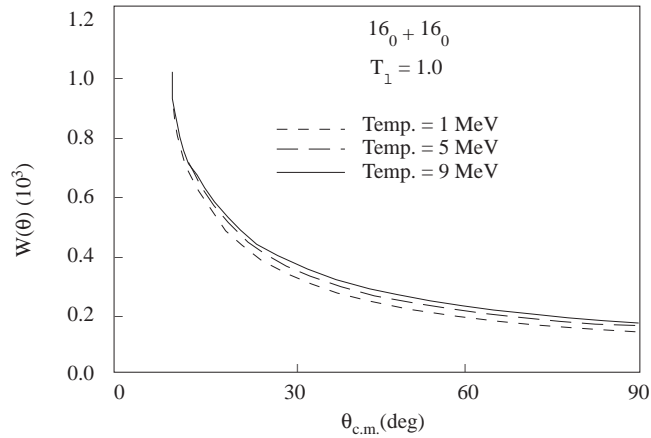


Figure 2. Angular distributions of alpha fragments from the $16_0 16_0$ reaction for various values of the nuclear temperature.

fission system are proportional to the fission cross sections that increase by increasing it as shown in Figures 1 and 2. In both figures, $W(\theta)$ are found very close for different temperatures at low value of the angle θ of about $\theta = 15$ degrees. For values of θ less than 15 degrees, $W(\theta)$ for the low temperature of $T = 1MeV$ is found to be larger than that for the largest temperatures of $T = 5MeV$ and $9MeV$. However, for values of θ larger than $\theta = 15$ degrees, the proportionality is found to be increased and $W(\theta)$ is smaller for low temperatures than for larger temperatures. Also, we notice that $W(\theta)$ slows

down faster for low temperatures than for the other cases of larger temperatures with $T = 5MeV$ and $9MeV$. The same calculations are done for the ratios of $W(\theta)/W(90)$ versus the angle θ for different values of the temperatures, which are introduced in Figure 3. It is found that the fission fragment angular distributions are normalized to one at $\theta = 90$. The calculations are extended to $\theta = 170$ and is introduced in Figure 4. From the calculations shown in Figure 4, we see that the results are symmetric around the angle $\theta = 90$. It is noticed that when the temperature $T = 1MeV$, then the angular distribution follows $a \frac{1}{\sin \theta}$ distribution for all angles θ greater than 10. Also, when the temperature is increased to $T = 2MeV$, the angular distribution follows $a \frac{1}{\sin \theta}$ distribution for angles θ greater than 15. Consequently, we find that as the temperature is increased, the $\frac{1}{\sin \theta}$ distribution is found for larger values of θ . This result is in agreement with the previous results [13] for angular distributions of fragments from fission induced by $220MeV$ ^{20}Ne on targets of ^{165}Ho , ^{197}Au and ^{209}Bi .

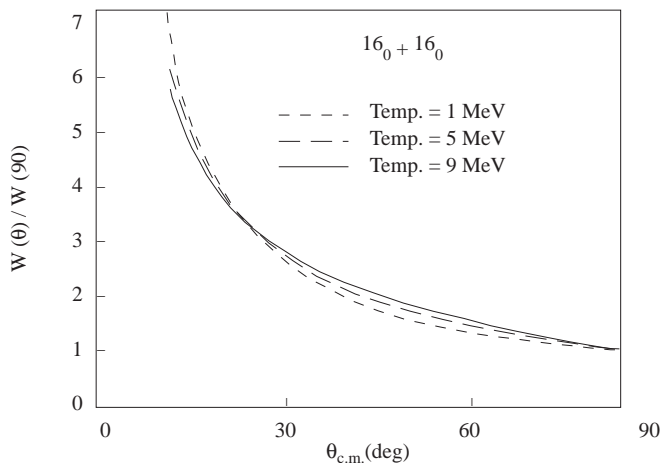


Figure 3. Angular distributions of alpha fragments from the $^{16}O + ^{16}O$ reaction for various values of the nuclear temperature.

The ratios of the angular distributions $W(\theta)/W(90)$ are plotted against the temperature T for different values of the angle θ and introduced in Figure 5. In this Figure 5, we noticed that the values of $W(\theta)/W(90)$ are much larger for $\theta = 10$ than that for the other θ values of $\theta = 30$ to $\theta = 90$. At $\theta = 10$, the dependence of $W(\theta)/W(90)$ on the temperature T is very small and remains so until nearly $3MeV$. For greater values of temperature greater than $3MeV$, the values of $W(\theta)/W(90)$ are found to decrease. On the other hand, for values of $\theta = 30$ to 70 degrees the values of $W(\theta)/W(90)$ increase by increasing the temperature T . However, at $\theta = 90$, the fission fragment angular distributions are normalized to unity for all values of the temperature T . At a value of the temperature $T = 1MeV$, the angular distributions $W(\theta)$ are calculated as a function of

FARAG

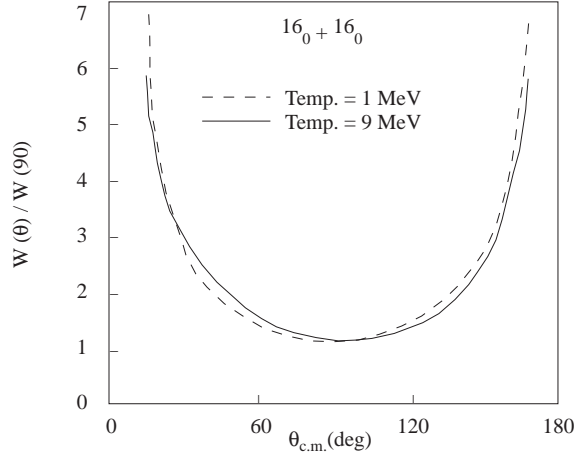


Figure 4. Angular distributions of alpha fragments from the $^{16}\text{O} + ^{16}\text{O}$ reaction for various values of the nuclear temperature.

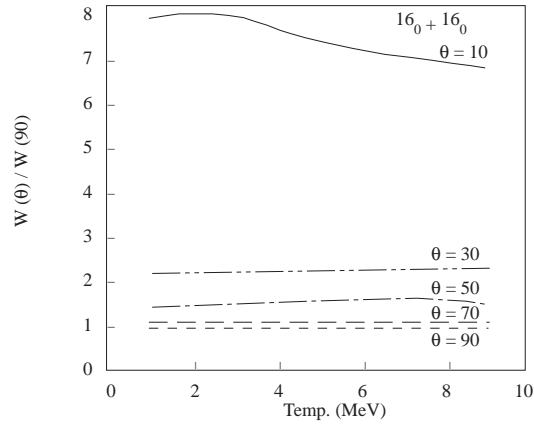


Figure 5. Dependence of the angular distributions of the alpha fragments from the $^{16}\text{O} + ^{16}\text{O}$ reaction on nuclear temperatures calculated for various values of the angle θ .

the angle θ for different values of the transmission factor T_ℓ ranging from $T_\ell = 0.2$ to $T_\ell = 1$. The results of the calculations are shown in Figure 6 for θ from 10 to 170 and in Figure 7 for θ from 10 to 90. The largest values of $W(\theta)$ are near angle $\theta = 10$ while the lowest (values of $W(\theta)$ are near angle $\theta = 10$ while the lowest) values are at $\theta = 90$. From Figure 6, we see that the values of $W(\theta)$ are symmetric around the angle $\theta = 90$. The values of the variances S_0^2 have been calculated for different values of the temperature from $T = 1\text{MeV}$ to $T = 9\text{MeV}$, and are shown in Figure 8. The obtained values of

FARAG

the calculated variance S_0^2 for different values of the nuclear temperature are listed in Table 1 for different values of the center of mass energy. Figures 1-8 show the effects of the different values of different parameters considered in the present work; as the nuclear temperature, incident energies, transmission coefficients and the angular distributions that extended from forward direction $\theta \approx 10^\circ$ to the backward direction $\theta \approx 170^\circ$.

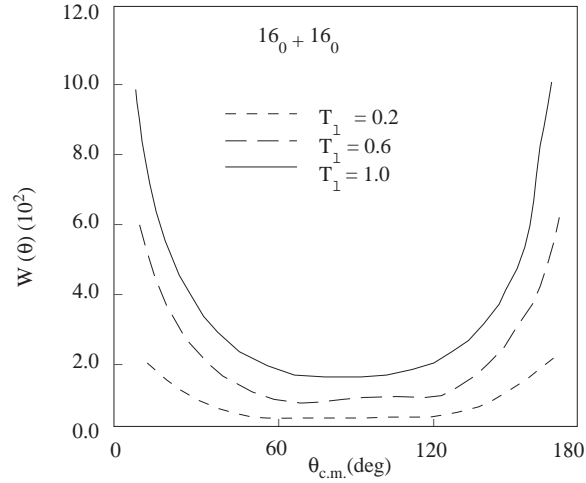


Figure 6. Angular distributions of alpha fragments from the $^{16}\text{O} + ^{16}\text{O}$ reaction for various values of the transmission coefficient.

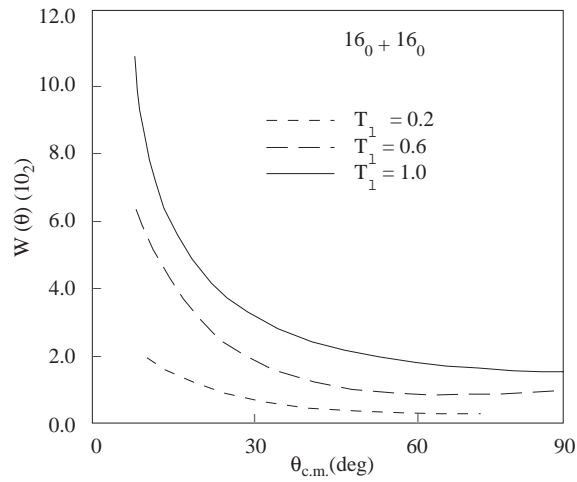


Figure 7. Angular distributions of alpha fragments from the $^{16}\text{O} + ^{16}\text{O}$ reaction for various values of the transmission coefficient.

FARAG

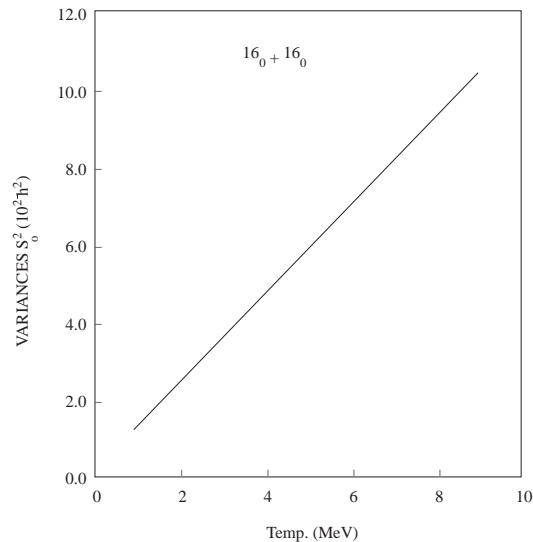


Figure 8. The variance of alpha fragments from the $^{16}O + ^{16}O$ reaction and their dependence on the nuclear temperature.

4. Discussion and Conclusions

In the present work, the multifragmentation of heavy ion induced fission is considered following the statistical scission model. The oxygen-oxygen reactions which result in a product sequence of eight alpha particles have been studied. Numerical calculations have been carried out for the angular distributions of the fission fragments for different incident energies and different nuclear temperatures. The results show that the angular distributions strongly depend on the nuclear temperatures and have symmetric behaviour around the angle $\theta = 90^\circ$. The dependence on the nuclear temperatures is shown to be important also for the effective variances. These results are in good agreement with previous calculations [14].

Therefore one can conclude that the statistical scission model is very suitable for calculating the multifragmentation of heavy ion induced fission.

Acknowledgement

I am very thankful and grateful to Prof. Ahmed Osman for his kind and valuable discussions and comments.

FARAG

References

- [1] A. Yokoyama, W. Loveland, J.O. Liljenzin, K. Aleklett, D.J. Morrissey and G.T. Seaborg, *Phys. Rev.*, **C46** (1992) 647.
- [2] W.W. Wilcke, J.R. Birkelund, H.J. Wollersheim, A.D. Hoover, J.R. Huizenga, W.U. Schrder and L.E. Tubbs, *At. Data Nucl. Data Tables*, **25** (1980) 391.
- [3] B.B. Back, *Phys. Rev.*, **C31** (1985) 2104.
- [4] H. Rossner, J.R. Huizenga and W.W. Schrder, *Phys. Rev.*, **C33** (1986) 560.
- [5] S. Cohen, F. Plasil and W.J. Swiatecki, *Ann. Phys. (N.Y.)*, **82** (1974) 557.
- [6] A. Gavron, P. Eskola, A.J. Sierk, J. Boissevain, H.C. Britt, K. Eskola, M.M. Fowler, H. Ohm, J.B. Wilhelmy, S. Wald and R.L. Ferguson, *Phys. Rev. Lett.*, **52** (1984) 589.
- [7] T. Ericson, *Adv. Phys.*, **9** (1960) 425.
- [8] H.H. Rossner, J.R. Huizenga and W.U. Schrder, *Phys. Rev. Lett.*, **53** (1984) 38.
- [9] V.E. Viola, Jr., *At. Data Nucl. Data Tables*, **1** (1966) 391.
- [10] P.D. Bond, *Phys. Rev. Lett.*, **52**(1984) 414.
- [11] P.D. Bond, *Phys. Rev.*, **C32**(1985) 471.
- [12] P.D. Bond, *Phys. Rev.*, **C32**(1985) 483.
- [13] H. Rossner, D. Hilscher, E. Holub, G. Ingold, U. Jahnke, H. Orf, J.R. Huizenga, J.R. Birkelund, W.U. Schrder and W.W. Wilcke, *Phys. Rev.*, **C27** (1983) 2666.
- [14] A. Osman and M.Y.H. Farag, *I1 Nuovo Cimento*, **108A** (1995) 155.